E-proceedings of the 36th IAHR World Congress
28 June – 3 July, 2015, The Hague, the Netherlands

AIR ENTRAINMENT AND PRESSURE DEVELOPMENT IN SKIMMING FLOW ON AN ABRUPT SLOPE CHANGE ON STEPPED SPILLWAYS

M.J. OSTAD MIRZA[(1,2)], J. MATOS[(2)] , M. PFISTER[(1)] & A.J. SCHLEISS[(1)]

[(1)] *Laboratory of Hydraulic Constructions, Ecole Polytechnique Fédérale de Lausanne, Lausanne, Switzerland,*
mohammadjavad.ostadmirza@epfl.ch
michael.pfister @epfl.ch
anton.schleiss@epfl.ch
[(2)] *Department of Civil Engineering, Architecture and Georesources, Instituto Superior Técnico, University of Lisbon, Lisbon, Portugal.*
jorge.matos@tecnico.ulisboa.pt

ABSTRACT

Numerous stepped spillways were built to date, namely on RCC gravity dams or on valley flanks besides embankment or rockfill dams, while some others are currently under design or construction. In some cases, slope changes may be required on stepped chutes, due to the topography, leading to reduced excavation and related economic benefits. A quite limited number of stepped spillways have been built with slope changes, whereas no systematic scientific investigation for designing such type of configuration has been conducted to date. Thus, there is a lack of information with regards to the main flow features along abrupt slope changes on stepped spillways. The present study is focussed on an experimental investigation of the air entrainment and pressure development on skimming flow on stepped spillways, in the vicinity of an abrupt slope change. Physical modelling was conducted in a relatively large scale facility, where detailed air-water flow measurements were gathered upstream and downstream of a 50˚-30˚slope change. In addition, dynamic pressure measurements were obtained on both vertical and horizontal faces of several steps in the vicinity of the slope change. The results on the air entrainment and pressure development are presented and discussed. A substantial influence was observed on the air entrainment and pressure development pattern, in comparison with typical results for constant sloping stepped spillway flows.

Keywords: Stepped spillways, Slope change, Skimming flow, Air entrainment, Pressure distribution.

1. INTRODUCTION

A significant number of stepped spillways were built in the last decades, namely those linked to the application of the roller compacted concrete (RCC) construction technique (e.g., Chanson, 2001, Frizell, 2006). Stepped spillways have also been built in combination with embankment and rockfill dams, namely on valley flanks adjacent to the dam, where slope changes may naturally occur, due to topography and economic reasons. Despite some few exceptions, such as the Upper Stillwater dam in the USA (Houston, 1987) and lower Siah-Bishe dam in Iran (Baumann et al., 2006), most stepped spillways have been designed for a constant chute slope.

Even though extensive research has been conducted so far on the hydraulics of conventional stepped spillways (e.g., Minor and Hager, 2000, Chanson, 2001, Frizell, 2006), stepped spillways with macro-roughness (e.g., André, 2004; André et al., 2004; Gonzalez et al, 2008; Bung and Schlenkhoff, 2010), or with non-uniform step heights (e.g., Felder and Chanson, 2011), there is presently insufficient information available on the flow behaviour on abrupt slope changes on stepped spillways.

The purpose of the present research is to study the effect of abrupt slope changes on the flow properties in skimming flow on stepped spillways. Experiments were conducted under different geometric and flow conditions. Results on air entrainment and pressure development in the vicinity of slope change region are presented and discussed.

2. EXPERIMENTAL SETUP

The experimental data were collected on a steep channel at the Laboratory of Hydraulic Constructions (LCH), EPFL, Lausanne. The channel consisted of four 2 m long and 0.5 m wide modules, with a 0.6 m high transparent sidewall to allow for flow observation. The channel was divided in two separated parts of different slopes, each of those including two modules of 4 m length (Fig. 1). The bottom slope of the upstream chute (i.e. pseudo-bottom angle) was set to φ=50º (1V:0.84H), while the downstream slope was set to φ=30º (1V:1.7H). The vertical step height was equal to h = 0.06 m. In total, 41 and 34 steps were provided along the 50 º and 30 º chutes, respectively. Along the 30º chute, 23 steps were included the test reach for the air concentration measurements. To allow for an independent variation of the inflow depth

(d_0) and Froude number (F_{r0} = $q_w/(gd_0^3)^{1/2}$, where g is the gravitational acceleration), a jet-box was inserted at the upstream end of the channel. The maximum opening of the jet-box was 0.12 m, which was designed for a maximum unit discharge of 0.48 m^2/s. An electromagnetic flow meter was used to measure the discharge with an accuracy of 1% full span, corresponding to a discharge of 3 l/s. By using the jet-box, the pressurized pipe approach flow was transformed into a free surface flow. As a result of such system, the location of the inception of air entrainment was shifted upstream and the developing region of the flow was shorten, in comparison with those for a free-overflow upstream control. For the range of step geometries and discharges, quasi-uniform flow conditions were reached on the upstream slope. The test program included a series of observations and measurements for unit discharges ranging between 0.2 m^2/s (d_c/h = 2.6) and 0.46 m^2/s (d_c/h = 4.6) with d_c = critical flow depth and h= step height. For such flow rates, corresponding to the skimming flow regime, the Reynolds number ($R_e = q_w/\upsilon$) varied between 1.9×10^5 and 4.6×10^5, and the minimum inflow Weber number at the exit of the jet-box ($W_{e0} = V_{m0}/(\sigma \sin\varphi/\rho h)^{1/2}$) varied between 124 and 189, where υ is the kinematic viscosity of water, V_{m0} is the inflow depth averaged velocity at the exit of the jet-box ($V_{m0} = q_w/d_0$), σ is the interfacial surface tension, and ρ is the water density (Table 1). For such geometric and flow conditions, scale effects are expected to be negligible (e.g., Boes and Hager, 2003, Pfister and Chanson, 2014).

(a) (b)

Figure 1. Physical model of the stepped spillway with an abrupt slope change at LCH-EPFL: a) General view, and dual fiber-optical probe mounted on an automatic positioning system in operation; b) Side view of the configuration associated to test number 2 (see Table 1), where some step numbers are indicated.

The measurements of the air–water flow properties were conducted at various streamwise cross-sections along the stepped spillway. For the present paper, a limited number of steps were analyzed, near the transition region (steps -3 to +3) (Fig. 1). The profiles were measured in each cross-section perpendicular to the pseudo-bottom, including 30 points from about 5 mm distance to the step edge up to the flow surface, with 0.01 m point spacing.

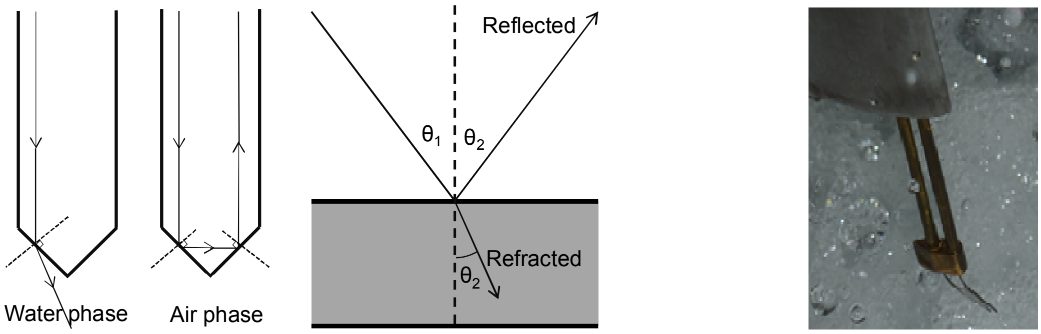

(a) (b)

Figure 2. Dual fiber-optical probe developed by RBI, used at LCH-EPFL: (a) schematic of the measuring principle; (b) photograph of the double fiber-optical probe in operation.

Table 1 Test conditions.

Test no.	h (m)	d_0 (m)	q_w (m^2/s)	d_c/h (-)	R_e(-)×10^5	F_{r0}(-)	W_{e0} (-)
1	0.06	0.082	0.47	4.6	4.6	6.4	189
2	0.06	0.093	0.35	3.8	3.4	4.0	124
3	0.06	0.045	0.20	2.6	1.9	6.7	146

A dual fiber-optical probe including two sapphire tips of 0.1 mm diameter, with a streamwise distance of 2 mm and a sampling rate of 1 MHz developed by RBI Instrumentation, France, was mounted on an automatic positioning system for measuring the air concentration (Figs. 1 and 2). The measurement principle is based on the Snell's law of optics. According to different refraction indices between the sapphire tips and the surrounding air–water phase, an infrared light supplied from an opto-electronic device to the tip is reflected and detected if the tip is positioned in the air-phase, while it is refracted and lost in the water-phase (Fig. 2). After signal amplification, this system delivers crenel type voltage outputs, in which high and low parts corresponds to air and water phase respectively (Chaumat et al., 2007). This probe measures the totally conveyed air concentration, without any distinction between entrapped and entrained air (e.g., Pfister and Hager, 2011). The local air concentration C of the two-phase air–water flow resulted from an acquisition period of 25 s. The pressure measurements were collected along the vertical and horizontal face of steps in vicinity of slope change, as well as on two steps of near the downstream end. The measurements have been carried out using piezoresistive pressure transmitters of Keller-druck PR-23/8465.2 with measurement frequency of 1 kHz and range of -0.1 to 0.2 bar. The mean, 95th and 5th percentiles of pressure were obtained from acquisition periods of 70 s. The pressure transducers were mounted on both vertical and horizontal step faces as shown in Figs. 3 and 4. Therein the values of z/h are equal to 0.30, 0.55 and 0.70, irrespective of the chute slope (z is the distance from the step edge, along the vertical face, and h is the step height: h=0.06 m); x/l is equal to 0.35 and 0.64, for the 50º slope, and 0.17, 0.50, and 0.84, for the 30º slope (x is the distance from the step edge, along the horizontal face, and l is the step length: l=0.050 m and 0.104 m for the 50º and 30º slopes, respectively).

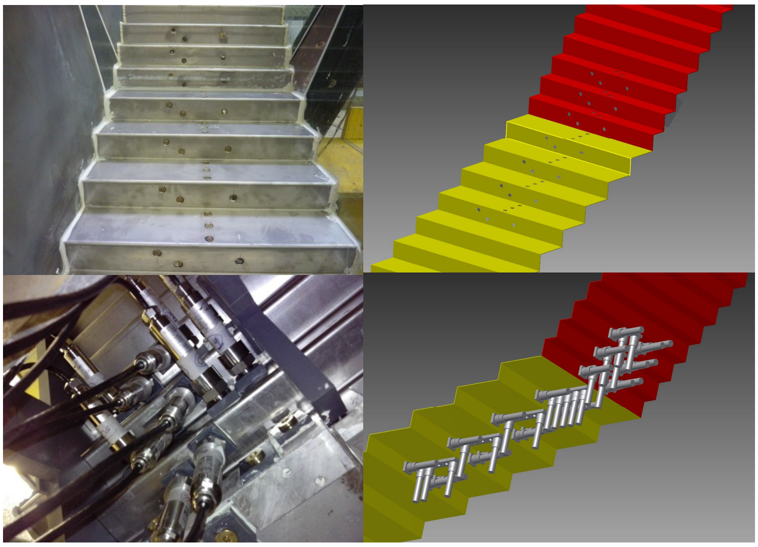

Figure 3. Pressure transducers installed in the vicinity of the slope change: photographs (left side) and schematics (right side) of the 50º-30º slope change equipped with pressure transducers.

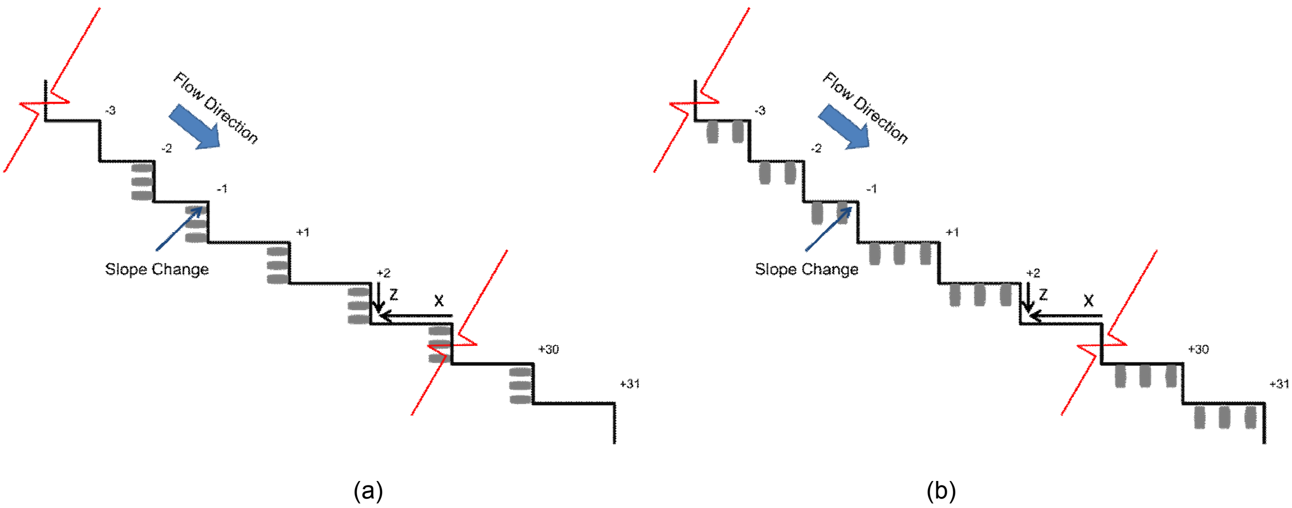

Figure 4. Schematic of the pressure transducers installed on the vicinity of slope change (step numbers -3 to +2) as well as near the downstream end (step numbers +30 and +31): a) vertical step faces; b) horizontal step faces.

3. AIR-WATER FLOW PROPERTIES ALONG THE SLOPE CHANGE REGION

3.1 Air concentration

The local air concentration *C* is defined as the time-averaged value of the volume of air per unit volume of air and water. Figure 5 shows measured air concentration profiles versus normalized depth at various step edges, upstream and downstream of the 50˚-30˚ slope change, for d_c/h=3.8. The air concentration was found to decrease from the quasi equilibrium profile when approaching the slope change cross-section, for identical distance to the pseudo-bottom (see Fig. 5a, steps -3 to -1 versus the advection-diffusion model for the air bubbles by Chanson, 1997); in contrast, the air concentration generally increases shortly downstream of the slope change (steps +1 to +3, Fig. 5b), particularly from step +2 to +3 (except near the pseudo-bottom), evolving from a S-shape distribution towards a more stretched profile. This is expected to be due to the higher pressures near the pseudo-bottom and flow curvature reversal in the vicinity of the slope change (Fig.1).

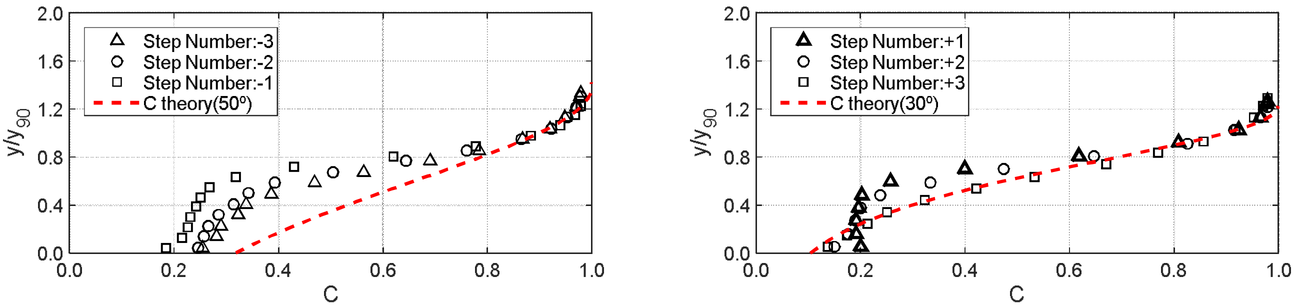

(a) (b)

Figure 5. Air concentration distribution a) upstream and b) downstream of the slope change, for d_c/h =3.8 ("-" and "+" signs represent the steps upstream and downstream of the slope change, respectively (step numbers as per Figs.1, 4); Note: C theory – as per Chanson (1997), for uniform flow on a similar sloping chute.

The development of the air concentration profiles along the slope change region is not significantly influenced by the relative critical depth, as shown in Fig. 6. Similarly to the analysis of Fig. 5b, the shape of the air concentration distribution for step +3 is markedly different than those corresponding to the upstream steps, regardless of the critical depth.

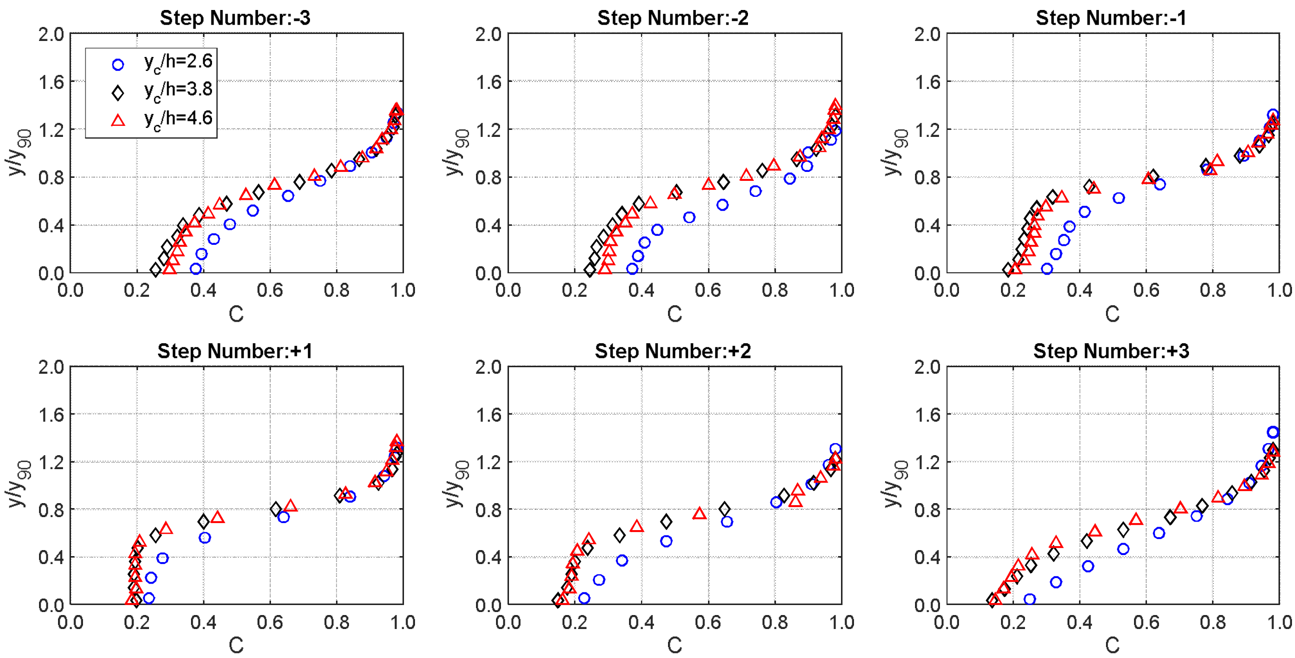

Figure 6. Air concentration distribution in the vicinity of the slope change, for various discharges ("-" and "+" signs represent the steps upstream and downstream of the slope change (step numbers as per Figs. 1, 4).

The streamwise distribution of the characteristic flow depths of (Y_{90}, Y_{95}, Y_{99}) upstream and downstream of the slope change are included in Fig. 7. For step numbers -9 to -1, the characteristic depths Y_{90} *and* Y_{95} remain practically constant (Fig. 7a), whereas flow bulking is noticeable downstream of step +2 (Fig. 7b). A clear reversal in the flow curvature is noticeable on such step, as previously suggested from the analysis of Figs. 5 and 6.

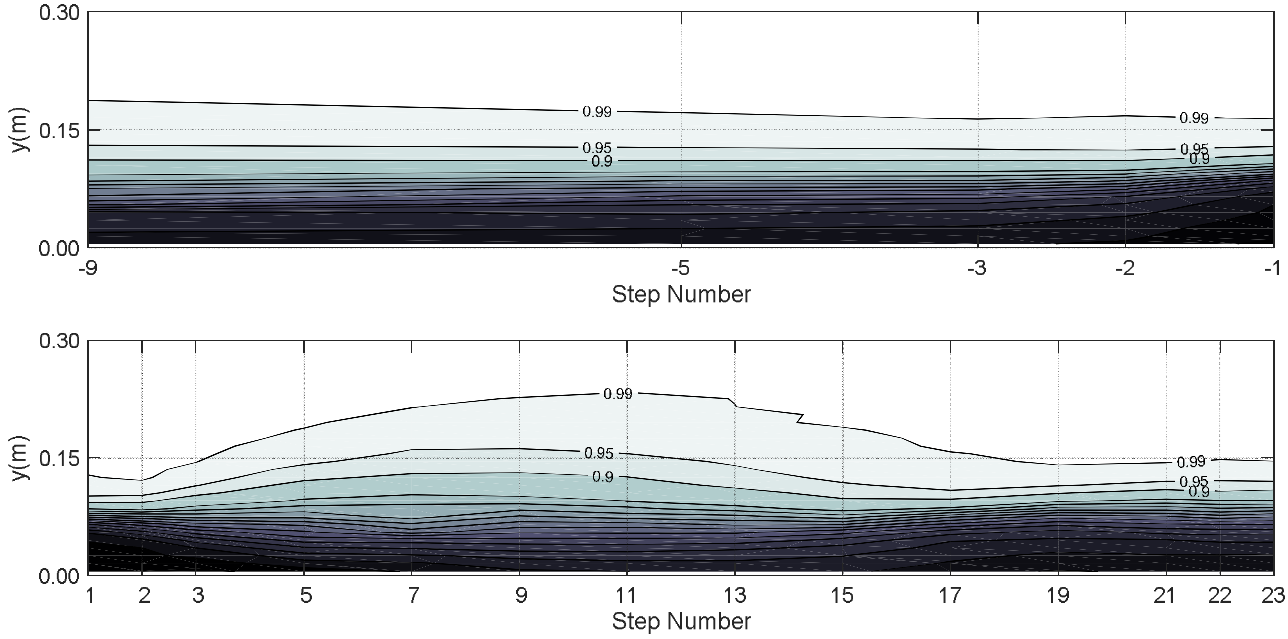

Figure 7. Typical air concentration contour: a) upstream, and b) downstream of the slope change for d_c/h =3.8 (y is flow depth perpendicular to the pseudo-bottom).

3.2 Pressure development

The evaluation of the dynamic pressures on the steps is important for the design of stepped spillways, as addressed in numerous investigations to date (e.g., Houston, 1987, Matos et al., 2000, Mateos and Elviro, 2000, Sánchez-Juny et al., 2000, 2007, Amador et al., 2009).

Figure 8 includes the mean, 95th and 5th percentiles of the dynamic pressure (normalized) on the horizontal step faces in the vicinity of the slope change. Both the mean and the 95th percentile show that the pressure tends to increase in the direction of the step edge, essentially due to the influence of the impact of the flow on the horizontal tread. Similar conclusions were obtained by Sánchez et al. (2007) and André and Schleiss (2008), for 50º and 30º sloping stepped chutes, respectively. Considerably larger values of the mean and 95th pressure percentiles were found immediately after the slope change (Fig. 8b). On the other hand, a relatively small influence of the pressure tap location is observed for the 5th percentile.

The streamwise development of the maximum and minimum spatial values (on each horizontal step face) of the mean, 95th and 5th percentiles of the dynamic pressure are shown in Fig. 9. The influence of the slope change on those pressures are initiated slightly upstream of the slope change. A significant increase in the pressure occurs in the vicinity of the slope change (Fig. 9, from steps -2, -1 to steps +1, +2). Further downstream, the pressure decreases significantly, and the values at the downstream end of the chute are of the same order of magnitude as those upstream of the slope change.

The mean, 95th and 5th percentiles of the dynamic pressure on the vertical step faces, in the vicinity of the slope change, indicate a small influence of the location of the pressure tap, for z/h ranging from 0.3 to 0.7 (Fig.10). Negative values of the 5th percentile values were also found, regardless of the step number.

The streamwise development of the maximum and minimum spatial values (on each vertical step face) of the mean, 95th and 5th percentiles of the dynamic pressure are shown in Fig. 11. A considerable increase of both maximum and minimum pressures occurs in the vicinity of the slope change. Such result would be expected, because of the small influence of the location of the tap on the magnitude of the pressure, as per Fig. 10.

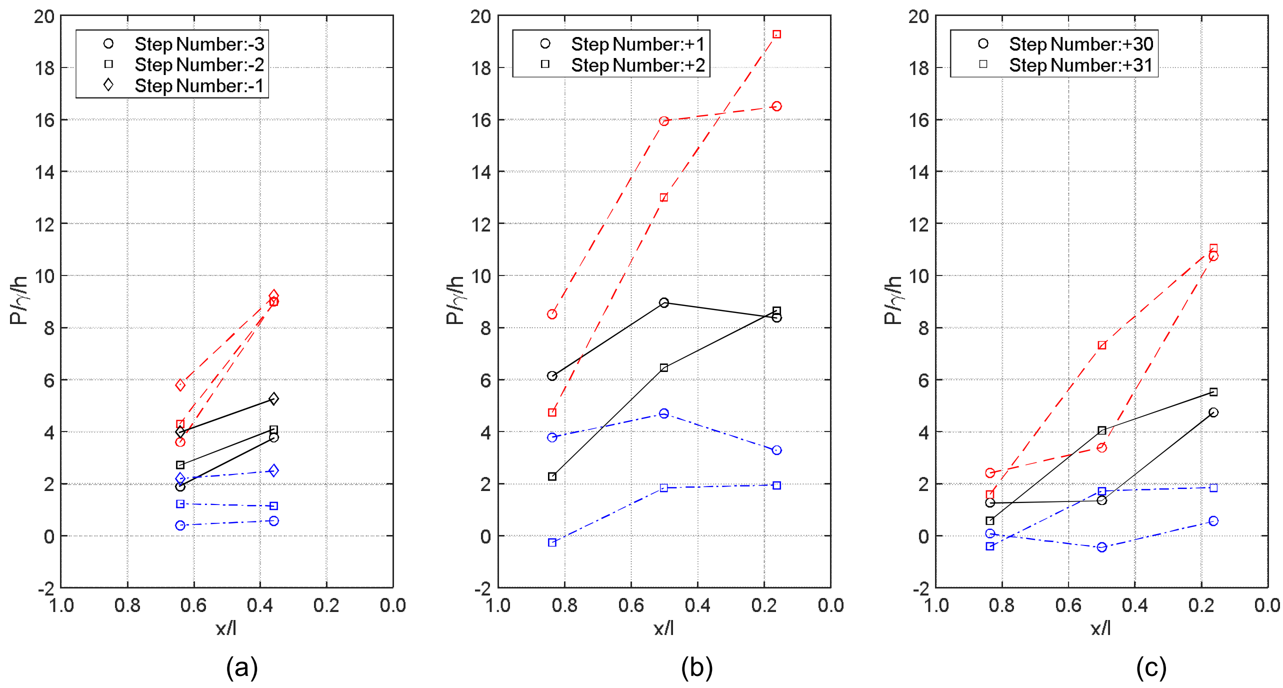

Figure 8. Mean (-), 95th (- -) and 5th (- .) percentiles of the dynamic pressure on the horizontal step faces, in vicinity of the slope change, and far downstream, for d_c/h =3.8; l is the step length and x is the distance from the step edge, along the horizontal face (see Fig.4).

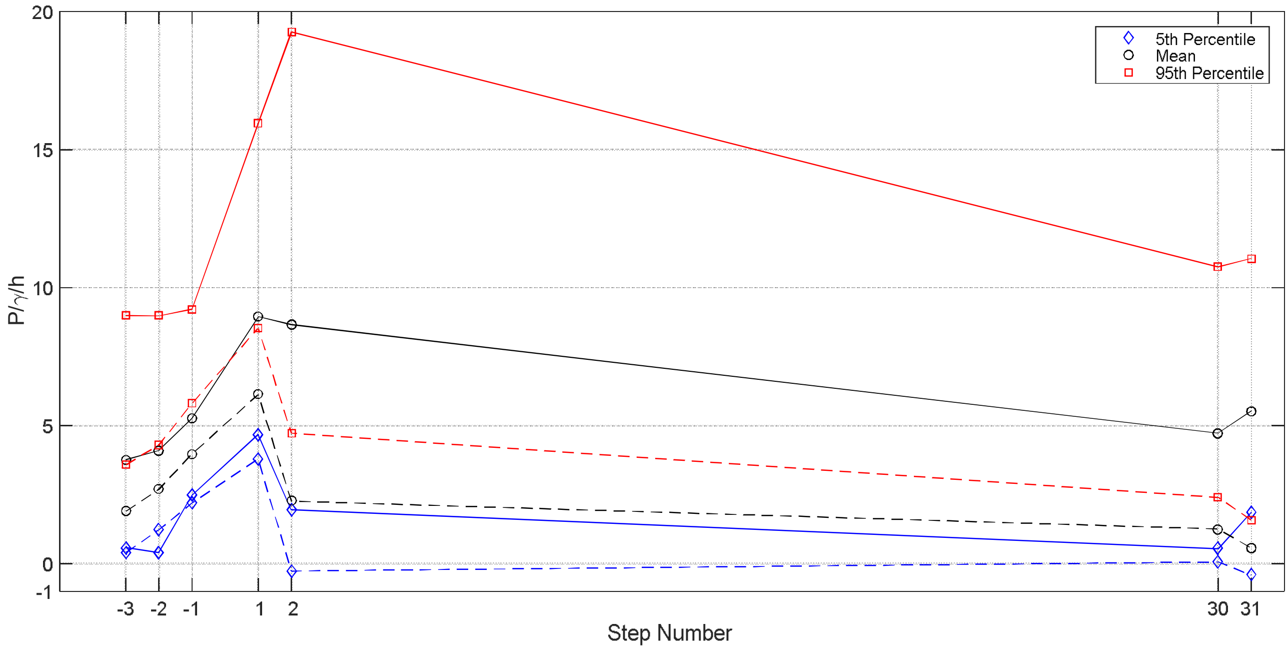

Figure 9. Maximum and minimum spatial values of the mean (- / --), 95th (- / --) and 5th (- / --) percentiles of the dynamic pressure on each horizontal step face in the vicinity of slope change, and far downstream, for d_c/h =3.8.

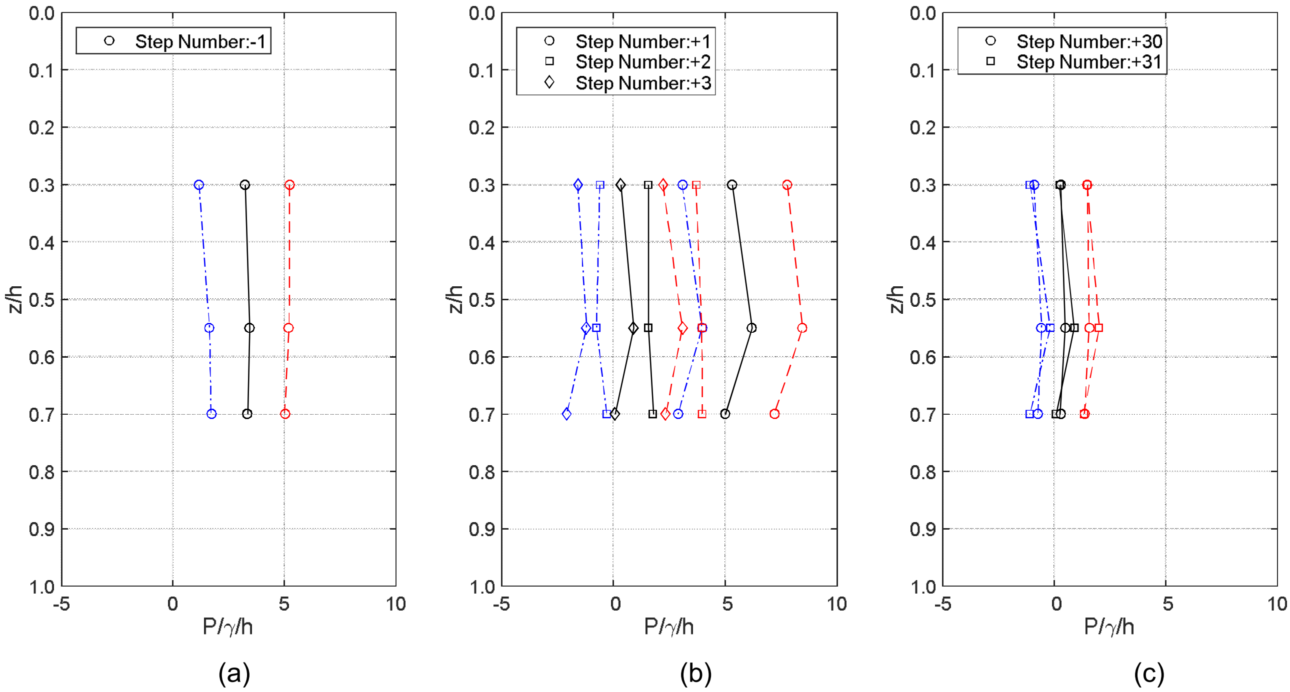

Figure 10. Mean (-), 95th (- -) and 5th (- .) percentiles of the dynamic pressure on the vertical step faces, in vicinity of the slope change, and far downstream, for d_c/h =3.8; h is the step height and z is the distance from the step edge, along the vertical face (see Fig.4).

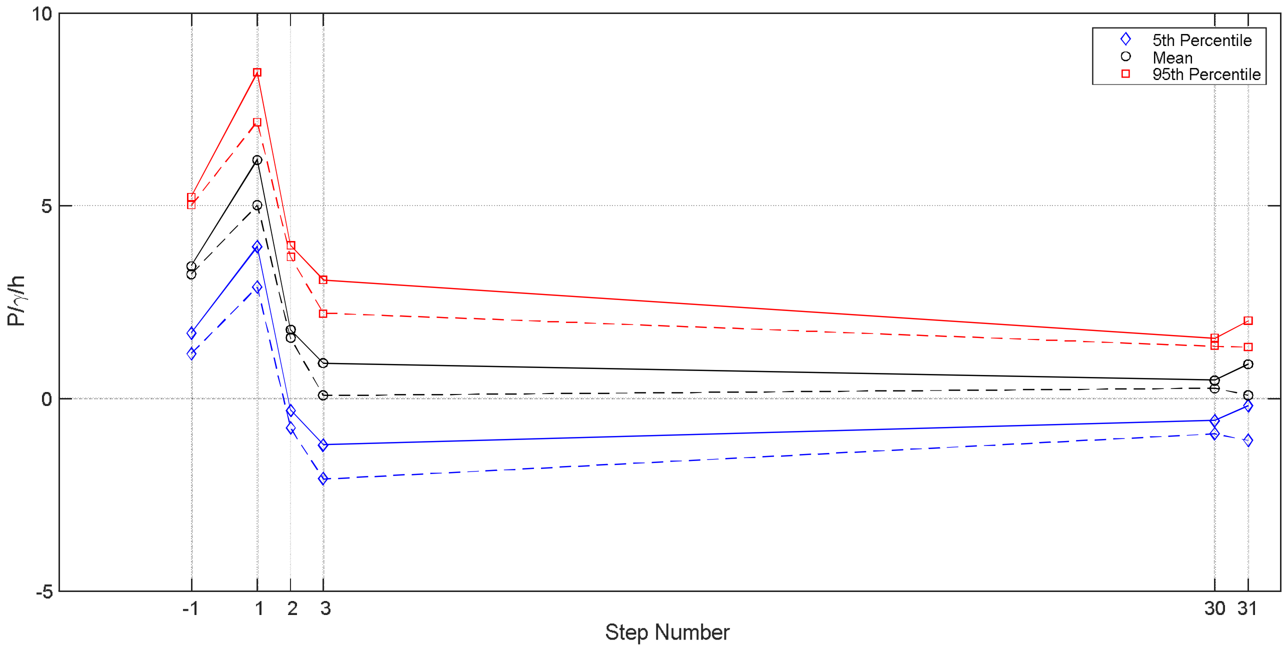

Figure 11. Maximum and minimum spatial values of the mean (- / --), 95th (- / --) and 5th (- / --) percentiles of the dynamic pressure on each vertical step face in the vicinity of slope change, and far downstream, for d_c/h =3.8.

4. CONCLUSIONS

In the present paper, the effect of an abrupt slope change on the air entrainment and pressure development in skimming flow on stepped chutes is analysed. Experimental tests were conducted at various cross-sections on a relatively large scale model of a 50º-30º abrupt slope change, assembled at the Laboratory of Hydraulic Constructions (LCH) of EPFL. Three sets of experiments were carried out for different Froude numbers and approach flow depths. The following conclusions can be drawn:

- In general, for identical distance to the pseudo-bottom, the air concentration decreases when approaching the slope change cross-section (departing from the quasi equilibrium profile), whereas it increases shortly downstream, but near the pseudo-bottom. Within the slope change region, the air concentration distribution evolves from a S-shape distribution towards a more stretched profile.
- The characteristic depths (e.g., Y_{90}) remain practically constant in the vicinity of the slope change, whereas a significant increase is noticeable further downstream, due to the strong flow curvature and bulking.
- Both the mean and the 95th percentile of the dynamic pressure on the horizontal step faces show an increasing value near the step edge; on the other hand, the mean, 95th and 5th percentiles of the pressure distribution on the vertical step faces are not significantly dependent on the tap location (for normalized distances z/h ranging from 0.3 to 0.7).
- A notable increase in the maximum and minimum spatial values of the mean, 95th and 5th percentiles of the dynamic pressure on the horizontal step faces occurs immediately downstream of the slope change, whereas the pressure decreases significantly further downstream. A similar trend is observed for the mean, 95th and 5th percentiles of the dynamic pressure on the vertical step face, even though with less pronounced maxima.

ACKNOWLEDGMENTS

The study was carried out in the framework of the IST-EPFL Joint Doctoral Initiative. The Ph.D. research has been granted by the Fundação para a Ciência e a Tecnologia (FCT), Portugal under grant SFRH/BD/51527/2011, and the Laboratory of Hydraulic Constructions (LCH) of EPFL, Switzerland.

REFERENCES

Amador, A., Sánchez-Juny, M. and Dolz, J. (2009). Developing Flow Region and Pressure Fluctuations on Steeply Sloping Stepped Spillways. *Journal of Hydraulic Engineering*, 135(12), 1092-1100.

André, S. (2004). High Velocity Aerated Flows over Stepped Chutes with Macro-Roughness Elements. *Thesis No. 2993, EPFL, and Communication LCH No. 20,* Ed. A. Schleiss, Lausanne, Switzerland.

André, S., Matos, J., Boillat, J.-L and Schleiss, A. (2004). Energy Dissipation and Hydrodynamic Forces of Aerated Flow over Macro-roughness Linings for Overtopped Embankment Dams. *in Yazdandoost, F., and Attari, J. (Eds) "Proc. of Int. Conf. on Hydraulics of Dams and River Structures"*, 26-28 April 2004, Tehran, Iran, Taylor&Francis Group, London, ISBN 90 5809 632 7, pp.189-196.

André, S. and Schleiss. A.J. (2008). Discussion of "Pressures on a stepped spillway", by Sánchez-Juny, M.Bladé, and E.Dolz, J., in *Journal of Hydraulic Research*, 46(4), 574-576, 2008.

Baumann A., Arefi F. and Schleiss A. (2006). Design of Two Stepped Spillways for A Pumped Storage Scheme in Iran. *Proceedings of the International Conference Hydro 2006, Maximising the benefits of hydropower*, Porto Carras, Greece (CD-ROM).

Boes, R. M., and Hager, W. H. (2003). Two-phase flow characteristics of stepped spillways. *Journal of Hydraulic Engineering*, 129(9), 661-670.

Bung, D.B. and Schlenkhoff, A. (2010). Self-aerated Skimming Flow on Embankment Stepped Spillways: The Effect of Additional Micro-roughness on Energy Dissipation and Oxygen Transfer. *Preprints of 1st European IAHR Congress*, Edinburgh, Flash-drive.

Chanson, H. (1997). Air Bubble Entrainment in Free Surface Turbulent Shear Flows. *Academic Press*, London.

Chanson, H. (2001). The Hydraulics of Stepped Chutes and Spillways. *Balkema*, Lisse, the Netherlands.

Chaumat, H., Billet-Duquenne, A.M., Augier, F., Matthieu, C., and Delmas, H. (2007). On the reliability of an optical fibre probe in bubble column under industrial relevant operating conditions. *Experimental Thermal and Fluid Science*, 31(6), 495-504.

Felder, S., and Chanson, H. (2011). Energy Dissipation Down a Stepped Spillway with Non-uniform Step Heights. *Journal of Hydraulic Engineering*, 137(11), 1543-1548.

Frizell, K.H. (2006). Research State-of-the-Art and Needs for Hydraulic Design of Stepped Spillways. *Hydraulic Laboratory Report HL-2005-06*, U.S. Department of the Interior, Bureau of Reclamation, Denver, Colorado, USA.

Gonzalez, C.A., Takahashi, M. and Chanson, H. (2008). An Experimental Study of Effects of Step Roughness in Skimming Flows on Stepped Chutes. *Journal of Hydraulic Research*, 46 (Extra Issue 1), 24-35.

Houston, K.L. (1987). Hydraulic Model Studies of Upper Spillway Dam Stepped Spillway and Outlet Works. *Report No. REC-ERC-87-6*, U.S. Department of Interior, Bureau of Reclamation, Denver, USA.

Mateos, C., Elviro, V., (2000). Stepped Spillway Studies at CEDEX, Proc. *Int. Workshop on Hydraulics of Stepped Spillways*. VAW, ETH Zurich, H.E. Minor and W.H. Hager (eds). Balkema, Rotterdam, 87-94.

Matos, J., Quintela, A., Sánchez-Juny, M. and Dolz, J. (2000). Air entrainment and safety against cavitation damage in stepped spillways over RCC dams. in Minor, H.-E. and Hager, W. (eds), *Proceedings of the International Workshop on Hydraulics of Stepped Spillways*, A.A. Balkema/Rottersam/Brookeld, Zürich, Switzerland, pp. 69-76.

Minor, H. E., and Hager, W. H., eds. (2000). Hydraulics of stepped spillways. *Balkema*, Rotterdam,The Netherlands.

Pfister, M. and Hager, W.H. (2011). Self-entrainment of Air on Stepped Spillways. *International Journal of Multiphase* Flow 37(2), 99-107.

Pfister, M., Chanson, H. (2014). Two-phase air-water flows: Scale effects in physical modelling. *Journal of Hydrodynamics*, 26(2), 291-298.

Sánchez-Juny, M., Pomares, J. and Dolz. J. (2000). Pressure Field in Skimming Flow over a Stepped Spillway. in Minor, H.E. and Hager, W.H. (Eds) *Preprints of the International Workshop on Hydraulics of Stepped Spillways*, Zürich, Switzerland, Balkema, 137-145.

Sánchez-Juny, M., Bladé, E. and Dolz, J. (2007). Pressure on a stepped spillway. *Journal of Hydraulic Research*, 45(4), 505–511.